Effects of Tropospheric Spatio-Temporal Correlated Noise on the Analysis of Space Geodetic Data

A. Romero-Wolf, C.S. Jacobs, J.T. Ratcliff

Jet Propulsion Laboratory/NASA, California Institute of Technology, Pasadena, CA
Contact author: A. Romero-Wolf,   e-mail: `Andrew.Romero-Wolf@jpl.nasa.gov`

Abstract

The standard VLBI analysis models the distribution of measurement noise as Gaussian. Because the price of recording bits is steadily decreasing, thermal errors will soon no longer dominate. As a result, it is expected that troposphere and instrumentation/clock errors will increasingly become more dominant. Given that both of these errors have correlated spectra, properly modeling the error distributions will become increasingly relevant for optimal analysis. We discuss the advantages of modeling the correlations between tropospheric delays using a Kolmogorov spectrum and the frozen flow assumption pioneered by Treuhaft and Lanyi. We then apply these correlated noise spectra to the weighting of VLBI data analysis for two case studies: X/Ka-band global astrometry and Earth orientation. In both cases we see improved results when the analyses are weighted with correlated noise models vs. the standard uncorrelated models. The X/Ka astrometric scatter improved by ∼10% and the systematic $\Delta\delta$ vs. δ slope decreased by ∼50%. The TEMPO Earth orientation results improved by 17% in baseline transverse and 27% in baseline vertical.

1. Introduction

Measurement errors in VLBI data have, until recently, been partially dominated by thermal noise, which is characterized by Gaussian uncorrelated random distributions. As a result, the correlated nature of error sources such as those induced by clocks and troposphere fluctuations have not often been given much consideration given that their contribution was often small compared to thermal errors. However, as the cost of recording bits goes down, we are seeing data rates increasing. In fact, we anticipate up to a factor of ten reduction in thermal errors in the near future due to increased data rates. As thermal noise contributions drop, correlated noise sources will increasingly begin to dominate the error budget. Thus now is an opportune time to review data analysis with correlated noise models. Section 2 will review the model of troposphere correlations developed by Treuhaft and Lanyi (1987). We then give its application to two case studies: section 3 on VLBI for global astrometry and section 4 on VLBI for Earth orientation.

1.1. Historical Context

Data Rates: Until the last few years, VLBI systems had been recording at a standard rate of 128 Mbps for over a decade. Recent Research & Development VLBI (RDV) runs with the VLBA have increased that to 256 Mbps gaining a $\sqrt{2}$ improvement in signal to noise ratio (SNR). The current VLBA default continuum rate is 512 Mbps gaining a total factor of two SNR improvement. Within about the past year, the Mark-5C system has demonstrated 2 Gbps fringes at the VLBA for a factor of 4 total SNR improvement. NASA's Deep Space Network (DSN) is also moving to Mark-5C with its 2 Gbps. Eventually Mark-5C with parallel recording to two disk packs will

achieves 4 Gbps. Finally, the Haystack Mark-6 recorder (Whitney *et al.*, this volume) can achieve 16 Gbps recording with short term 32 Gbps rates.

In summary, the recent rapid improvements in recording data rates means that there will be factors of 10 or more improvement in SNR the near future compared to previous decades. In addition to these SNR driven reductions in random errors, we expect that moving the digitization process from the back end (after long cable runs) to near the front end will greatly reduce systematics errors from temperature driven variations in filters and cables delays. The combined effect of these technology improvements will be to make significant improvements in instrumental errors in the near future.

WVRs: The impact of tropospheric turbulence on VLBI data has been probed with the JPL Advanced Water Vapor Radiometers (A-WVR). An experiment was performed with the DSN 8000 km Goldstone-Madrid baseline where each station had an A-WVR (Bar-Sever et al. 2007) monitoring the brightness temperature of the 22 GHz water line along the line of site. The antennas were observing a very strong source and measuring phase delay to reduce the thermal error contribution to negligible levels. The results of the experiment showed that including the observations of the A-WVR reduces the scatter of the delay residuals from 3mm to 1mm. Unfortunately the Advanced WVR costs ~$500K (U.S.) and they are not available at every station.

However, when lacking such direct tropospheric calibrations, we can strive to model the statistical properties of the correlated spectrum of troposphere fluctuations errors using Kolmogorov's (1941) theory of turbulence. This theory will be used to convert density fluctuations in tropospheric water vapor content into fluctuations in the observed delays. The spatial and temporal scales of the density fluctuations will determine the degree of troposphere induced correlation between delays at different stations.

The inclusion of correlated error models in the analysis of VLBI data is expected to improve results by more rigorously treating common mode error sources. For example, a large scale troposphere fluctuation might alter several sequential delay measurements by nearly the same amount. In such a case, the strongest information would be in the differences between delays while the sum of delays would be poorly determined. This is one example where a correlated noise model might improve the solution's performance.

2. Troposphere Correlated Noise Model

Kolmogorov's theory of turbulence provides a handle on the spatial scales of troposphere fluctuations. The structure function of a turbulent velocity $\mathbf{u}$ is defined as $D_{\mathbf{u}}(R) = \langle |\mathbf{u}(\mathbf{r} + \mathbf{R}) - \mathbf{u}(\mathbf{r})|^2 \rangle$ where $\mathbf{r}$ is a position in the sky and $\mathbf{R}$ is an offset vector. Kolmogorov (1941) used dimensional arguments to determine that the structure function is given by a power law $D_{\mathbf{u}}(R) = C\epsilon^{2/3}R^{2/3}$ where ϵ is the average energy dissipation of the medium and C is a medium independent constant. This result assumes only that the turbulence is locally isotropic and that $R > (\nu^3/\epsilon)^{1/4}$ where ν is the viscosity of the medium.

In Tatarskii (1961) the structure function for spatial variations of the refractivity $\chi = ($ index of refraction - 1 $)$ are determined based on the Kolmogorov (1941) theory of turbulence. This is given by $D_{\chi}(R) = C^2 R^{2/3}$ where the constant C is independent of spatial coordinates $\mathbf{r}$ and $\mathbf{R}$. Starting from this point Treuhaft and Lanyi (1987) translated the turbulent refractivity structure function into radio signal delay and delay rate structure functions. The electromagnetic wave delay (τ) observed at an antenna is obtained by integrating the refractivity along the path of propa-

gation. This relation naturally connects the structure function in refractivity D_χ to the structure function in delay D_τ. The covariance of delays measured at different stations due to troposphere fluctuations on VLBI data are determined directly from the structure function.

The delay structure function (Figure 1) behaves as a broken power law whose exponent depends on the antenna separation ρ relative to the effective height of the troposphere ($h \sim 2$ km). The break can be intuitively understood as the difference between delay fluctuations being influenced by many small scale scatterers when $\rho/h < 1$ rather then being influenced by a few large scale scatterers $\rho/h > 1$. The magnitude of the structure function depends on the elevation angle since this determines the amount of troposphere the electromagnetic wave has traversed.

The spatial dependence of the delay structure function can be translated to a temporal dependence via the frozen flow model. This assumes that the overall turbulent structure of the troposphere is shifted in time with the direction of the wind. The wind speed scales relevant to the frozen flow model are typically ~ 10 m/s. For all the mathematical details for the calculation of structure functions, variances, and covariances as well as examples with DSN data see Treuhaft and Lanyi (1987).

3. Case Study 1: X/Ka Extragalactic Reference Frame

Our goal in our two case studies is to determine whether, given the thermal error levels derived from data rates used in existing data, the inclusion of correlated troposphere errors yet make a difference in the data analysis. The first case study used the X/Ka extragalactic reference frame data set (Garcia-Miro *et al.*, 2012) consisting of 59 VLBI observing sessions from Jul. 2005 to Feb. 2012 which covered the full range of α, but δ only down to $-45°$ using NASA's Deep Space network antennas in Goldstone, CA, to Madrid Spain and to Canberra, Australia.

We made two X/Ka solutions: (1) data weighted by uncorrelated Gaussian noise and zenith troposphere breaks every $\sim$40 min. (2) data weighted by Treuhaft-Lanyi troposphere covariance added to the formal thermal noise and rather than following the standard practice of introducing troposphere breaks, we use only one troposphere parameter estimate for each station over a 24 hour period. The advantage of including troposphere covariance is the it re-defines χ^2 such that drifts are not penalized nearly as much. Also the number of free parameters is reduced from what would typically be done. Note that both solutions used the exact same data and exact same a priori modeling.

Our figure of merit for the estimated X/Ka source coordinates was the wRMS agreement with the international standard ICRF2 catalog (Ma *et al.*, 2009). Table 1 shows the improvements were found in the wRMS agreement for $\alpha \cos \delta$ and δ as well as for the slope $\Delta\delta$ vs. δ. We are highlighting the $\Delta\delta$ vs. δ results because we expect declinations to be more strongly influenced by troposphere effects, due to the fact that low declinations tend to be observed at lower elevations and thus are observed through thicker atmosphere profiles.

The solution weighted with tropospheric covariance improved the wRMS agreement with ICRF-2 by 7% over the solutions using uncorrelated Gaussian weighting. We note that while a 7% improvement seems rather modest, in order to gain a similar improvement by averaging over additional data would require $\sim$14% more data. Given that the X/Ka data set consists of almost 7 years of data that would imply taking almost another year of data to get the improvement we get from applying correlated tropospheric noise weighting. In this sense, the tropospheric covariance approach makes a significant improvement to the X/Ka analysis.

4. Case Study 2: TEMPO Earth Orientation Measurements

We now move on to our 2nd case study. JPL's Time and Earth Motion Precision Observations (TEMPO) program produces rapid turnaround VLBI measurements of Earth orientation in support of spacecraft navigation which requires extremely timely and accurate Earth rotation information. TEMPO uses the nearly East-West baselines from Goldstone, California to Madrid, Spain making it sensitive to the UT1-UTC component of earth orientation. Median thermal errors for this data set were 9.2 psec in delay and 6.0 fsec/sec in rate, making it reasonable to assume that non-thermal errors dominate. The data of 300 sessions set covered 13 Sep. 1998 to 14 Jan. 2012.

We compared two weighting schemes to account for errors in the TEMPO data.
(1) Gaussian diagonal noise with weights scaled as $1/\sin(elevation)$ and troposphere parameter breaks.
(2) Correlated troposphere noise with spatio-temporal dependence and just one zenith troposphere parameter per site per session.

Our truth model was JPL Kalman Earth Orientation Filter (KEOF) multi-technique combination (Chin et al, 2009; Ratcliff & Gross, 2011) customized to contain no TEMPO data and interpolated to the epochs of the 300 TEMPO measurements. The bias/rate/covariance adjustments to the TEMPO data were computed simultaneously using a multivariate Maximum-Likelihood-Estimate procedure.

We subtracted KEOF Earth orientation estimates from the two TEMPO analyses and then compared wRMS of residuals. Because TEMPO measurements are based on a single baseline, they only determine two of the three Earth orientation angles. The third angle is held by an a priori constraint. For purposes of comparing results, instead of using the traditional X, Y polar motion and UT1-UTC, we rotated our results into the natural coordinates of the TEMPO baseline where baseline transverse and vertical are the directions determined by the TEMPO data. For the baseline transverse direction, the correlated noise analysis improved the wRMS agreement from 355 to 295 μas or about 17%. For the baseline vertical direction, the correlated analysis improved the wRMS agreement from 564 to 467 μas or about 27%. The greater improvement in the vertical direction is consistent with our expectation that the troposphere modeling more strongly influences the baseline vertical.

5. Conclusions and Outlook

In this study we have argued that the ongoing trend toward higher data rates implies that thermal errors are trending toward being negligible. In turn, this implies that other noise sources such as troposphere and clocks will become increasingly dominant in space geodetic data types such as VLBI. Given that troposphere and clock noises have correlated spectra, new methods of analysis are called for. We have examined the Treuhaft-Lanyi model for troposphere noise. Applying that model to two cases studies, we have seen improved results in both cases indicating that there is promise in our correlated noise approach. We expect that as thermal error levels continue to decrease, the inclusion of troposphere covariance error models will show increasingly more significant improvements in analysis results.

4

References

[1] Bar-Sever, Y.E., *et al.*, 'Atmospheric Media Calibration for DSN,' Proc. IEEE, **95**, 11, 2180, 2007.

[2] Chin, T. M., R. S. Gross, D. II. Boggs, and J. T. Ratcliff, 'Dynamical and Observation Models in the Kalman Earth Orientation Filter,' JPL IPN Prog. Rept. , 42–176, Pasadena, CA., 15 Feb. 2009.

[3] Garcia-Miro, C., *et al.*, 'XKa Celestial Reference Frame,' Proc. IVS GM, Madrid Spain 2012.

[4] Kolmogorov, A.N., 'Dissipation of Energy in Locally Isotropic Turbulence,' *Doklady Akad. Nauk SSSR*, **32**, 16, 1941.

[5] Ma, C., *et al.*, eds.: Fey, Gordon, Jacobs, '2nd Realization of ICRF by VLBI,' IERS, Germany, 2009.

[6] Ratcliff, J.T., & R.S. Gross, 'Comb. Earth Orientation Meas.: SPACE2010,' JPL Pub. 11-15, 2011.

[7] Tatarskii, V.I., *Wave Propagation in a Turbulent Medium*, Dover, New York, 1961.

[8] Treuhaft R.N. & Lanyi, G.E., 'Effect of Dynamic Wet Troposphere on Radio Interferometric Measurements,' *Radio Science*, **22**, 251, 1987.

[9] Whitney, A., *et al.*, 'Mark-6 Next Gen VLBI Data System,' Proc. of IVS GM, Madrid, Spain, 2012.
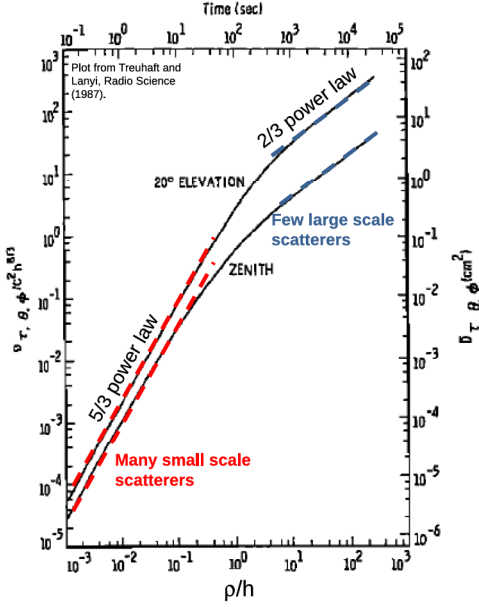
Figure 1: Delay structure function from Treuhaft and Lanyi (1987) is given by a broken power law whose exponent depends on the antenna separation ρ relative to the troposphere effective height (~ 1 km). See text for details.

Measure	No Trop. Cov.	Trop. Cov.
wRMS $\alpha \cos \delta$ (μas)	215	198
wRMS δ (μas)	300	283
$\Delta\delta$ vs. δ (μas/deg)	1.6 ± 1.0	1.1 ± 0.9

Table 1: Comparison of XKa catalog positions vs. ICRF2 for analysis with and without implementation of troposphere covariance error modeling.